JOURNAL OF APPLIED PHYSICS (2005) 98(5):53510.

Size-dependent change in interband absorption and broadening of optical plasma-resonance absorption of indium particles

Anno E, Tanimoto M

Size-dependent change in interband absorption and broadening of optical plasma-resonance absorption of indium particles

E. Anno[a] and M. Tanimoto
Department of Physics, Asahikawa Medical College, Asahikawa, Hokkaido 078-8510, Japan

(Received 13 September 2004; accepted 18 July 2005; published online 6 September 2005)

Optical absorption of indium-island films, consisting of indium particles smaller than about 500 Å in diameter, has been investigated experimentally. The interband absorption, the position of which is almost constant (at about 234 nm) irrespective of particle size, was found to disappear in particle sizes below about 200 Å in diameter. This disappearance is pointed out to be similar to that in lead particles, where the disappearance is due to the effect of surface atoms. Optical plasma-resonance absorption appeared at 276–335 nm. By simulating this absorption with a Maxwell-Garnett-type effective-medium theory, we investigated the relaxation time τ and the mean free path l of conduction electrons. τ and l for particle sizes of about 120 and 160 Å in diameter are estimated to be $(3.33\text{–}3.36)\times 10^{-16}$ s and 5.79–5.85 Å, respectively, which is smaller than the bulk values (0.38×10^{-14} s and 66.1 Å). The small τ and l are attributed to the scattering of the conduction electrons at lattice defects internal to the particles. © *2005 American Institute of Physics.* [DOI: 10.1063/1.2033151]

I. INTRODUCTION

Optical properties in transition from the atomic to the solid state are of fundamental interest in solid-state physics. Clusters and small particles represent a special state of matter intermediate between atoms and solids, so that they are well suited to study such optical properties. Metal particles smaller than the wavelength of incident light show interband absorption and/or optical plasma-resonance absorption caused by plasma oscillations of conduction electrons in the particles.[1]

Optical absorption of simple-polyvalent-metal particles has been studied only for lead[2] and aluminum particles,[3–5] which form island films. In lead particles,[2] the interband absorption, due to the transition from the initial state at the bottom of conduction bands, disappears in particle sizes below about 300 Å in diameter and before the disappearance its position is almost constant. This is because the density of state (DOS) at the lower portion of the conduction bands is decreased by the effect of surface atoms.[2] From the analysis of the optical plasma-resonance absorption of aluminum-island films, it has been reported[3,4] for aluminum particles that the relaxation time and mean free path of conduction electrons mainly depend on the scattering at lattice defects within the particles and are much smaller than the bulk values.

Indium is a simple-polyvalent metal with a body-centered-tetragonal (bct) structure. There is very little data on the optical absorption of indium particles. In the present study, we point out that the similarity to the interband absorption of lead particles[2] is important in the analysis of the interband absorption of indium particles. Based on the simulation of the optical plasma-resonance absorption of indium-island films consisting of indium particles, we investigate the relaxation time and mean free path of conduction electrons of the indium particles in a polycrystalline state.

II. TRANSMITTANCE

The transmittance formula for continuous thin metal film, the thickness d of which is smaller than the wavelength λ of incident light ($2\pi d \ll \lambda$), is applicable to metal-island film with a weight thickness d_w (which is the total volume of metal particles per unit substrate surface area)[6] smaller than $\lambda(2\pi d_w \ll \lambda)$.[7] In this case, when the metal-island film consists of metal particles which are the same shape and size (i.e., when there is no distributions of particle shape and size), the transmittance T for normal incidence of light can be expressed based on the Maxwell-Garnett-type effective-medium theory (EMT) as follows:[8]

$$T/T_s = \left[1 + \frac{2}{n_i + n_s}\frac{2\pi d_w}{\lambda}\varepsilon_a \frac{\Delta g}{(F+g)^2 + (\Delta g)^2}\right]^{-1}, \tag{1}$$

where n_i is the refractive index of the isotropic medium from which light is incident, n_s the refractive index of the isotropic transparent substrate, $T_s[=4n_i n_s/(n_i+n_s)^2]$ the transmittance for the bare surface of the substrate, ε_a the interparticle dielectric constant, and F the effective depolarization factor of the metal-island film. F includes the particle's depolarization factor, which depends on the particle shape, the dipole interactions between the particles, and the dipole interactions between the particles and their mirror images in the substrate.

As has been done in the present study, the ratio T/T_s can be measured directly with a double-beam spectrophotometer used with a bare substrate as reference sample. g and Δg in Eq. (1) are related to the dielectric constant ε_i of the metal particles by the relation[8]

$$g + i\Delta g = (\varepsilon_i/\varepsilon_a - 1)^{-1}. \tag{2}$$

[a]Electronic mail: anno@asahikawa-med.ac.jp

When ε_i consists of only the Drude equation with a plasma frequency ω_p and a relaxation time τ of conduction electrons, ε_i is expressed as[9]

$$\varepsilon_i = 1 - \omega_p^2/(\omega^2 + i\omega/\tau). \quad (3)$$

As is well known, τ depends on the scattering of conduction electrons.

In the optical plasma-resonance absorption of metal-island films, the absorption peak depends on d_w and τ, the position of the absorption peak depends on F, and the broadening (i.e., the plasma-oscillation damping), due to the scattering of conduction electrons, depends on τ.

III. EXPERIMENT

In a vacuum chamber, a fused-quartz substrate ($18\times18\times0.5$ mm^3) and electron-microscopic meshes covered with a carbon film were adjacently placed above an evaporation source. The distance (30.3 cm) from the evaporation source to the substrate equaled that to the meshes.

SiO_2 was first deposited both on the fused-quartz substrate and the meshes by electron-beam heating in an oil-free vacuum of $\sim10^{-8}$ Torr. Next, at pressures of $\sim10^{-7}$ Torr, indium (purity 99.9999%) was deposited in order to obtain island films. The films were then annealed for 1 h. During deposition and annealing, the substrate and meshes were maintained at a temperature of about 293 K. After annealing, the films were coated with SiO_2 (thickness 300–100 Å) to prevent adsorption or chemical reactions on exposure to air. The weight thickness and the deposition rate were monitored with a quartz-crystal oscillator. Transmittance of the evaporated SiO_2 film was almost constant within the spectral range of interest here.

Optical and electron-microscopic investigations were carried out after exposing the samples to air. With a double-beam spectrophotometer (Shimadzu UV-365), transmittance spectra for normal incidence and their first derivatives were measured in the wavelength range of 190–2500 nm at room temperature within the experimental accuracy of ±0.1% and ± [0.3(190 nm)–0.7(2500 nm)] nm. The first-derivative spectra were derived by computer applications where the first-derivative calculating function was convoluted to the transmittance spectrum divided at a wavelength interval (0.4–4.0 nm). The scale of the first derivative is variable (1–100). The best first-derivative spectrum was obtained when the wavelength interval was 4.0 nm. Thus, the first derivative in this paper is based on the change in the transmittance at 4.0-nm intervals. The particle size and electron-diffraction pattern were investigated with an electron microscope operating at 200 kV (Hitachi H-800). For simplicity, we assumed the particle shape, difficult to observe three dimensionally, to be spherical and estimated the particle diameter by regarding the length around the outside of the particle as the circumference. The particle-size distribution was shown in vol. %.

IV. RESULTS

A. Electron-microscopic investigation

Figures 1(a) and 1(b) show the electron micrographs of the indium-island films with particle diameters of about 440 and 160 Å, respectively. The indium particles display a complex contrast structure due to the diffraction contrast.[10] Thus, the indium particles are in a polycrystalline state, which is optically isotropic.

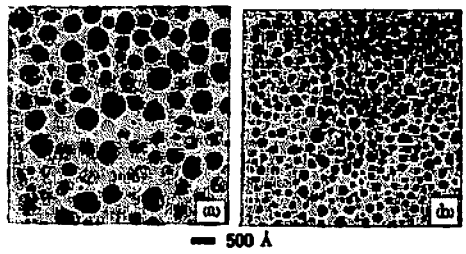

FIG. 1. Electron micrographs for the indium-island films with particle diameters of about (a) 440 and (b) 160 Å. The optical spectra and the particle-size distribution of the films (a) and (b) are shown in Figs. 2(b) and 3(a), respectively.

Only the bct structure could always be identified in electron-diffraction patterns of the films with particle diameters larger than about 100 Å, implying that the change of indium particles into compounds by chemical reactions occurred rarely. The electron-diffraction patterns were difficult to observe for films with particle diameters smaller than about 100 Å because of the low contrast due to the SiO_2 coating. Thus, we were not able to identify the crystal structure of indium particles smaller than this size. It has been reported[11] that indium particles smaller than about 50 Å in diameter have a cubic structure at a temperature of 120 K. We could not confirm such particles. Here, it is assumed that indium particles smaller than about 100 Å in diameter also have the bct structure.

We investigated the diameters of the (101) and (011) diffraction rings. There was little difference in the diameters between films with particle diameters of about 520, 220, and 120 Å. Thus, we concluded that contraction of lattice constants does not occur in indium particles larger than about 120 Å in diameter.

B. Spectrum of indium particles

In derivative spectra,[12] a step appearing in the first derivative shows the presence of absorption. Two steps were found below about 500 nm in the present study. Thus, spectra in a wavelength range of 190–1000 nm are shown in the present paper. The position of the maximum slope in the step corresponds to the position of the absorption peak.[12] In Figs. 2 and 3, the arrow indicates the position of the maximum slope, and the position of the absorption in the transmittance spectra is that indicated by the arrow.

The experimental spectra of the indium-island films with particle diameters of about 520, 440, 360, 260, and 220 Å are shown in Figs. 2(a)–2(e), respectively. The film of Fig. 2(b) is shown in Fig. 1(a). The position of the absorption is expressed below by $\lambda\pm\Delta\lambda$. This expression shows that the slope is at its maximum in the position range of $(\lambda-\Delta\lambda)$-$(\lambda+\Delta\lambda)$. The position of absorption 1 is (a) 235±3 nm, (b) 233±3 nm, (c) 233±3 nm, (d) 234±4 nm, and (e) 235±5 nm. Absorption 2 is positioned at (a) 335±5 nm, (b) 323±7 nm, (c) 314±6 nm, (d) 306±4 nm, and (e) 300±6 nm.

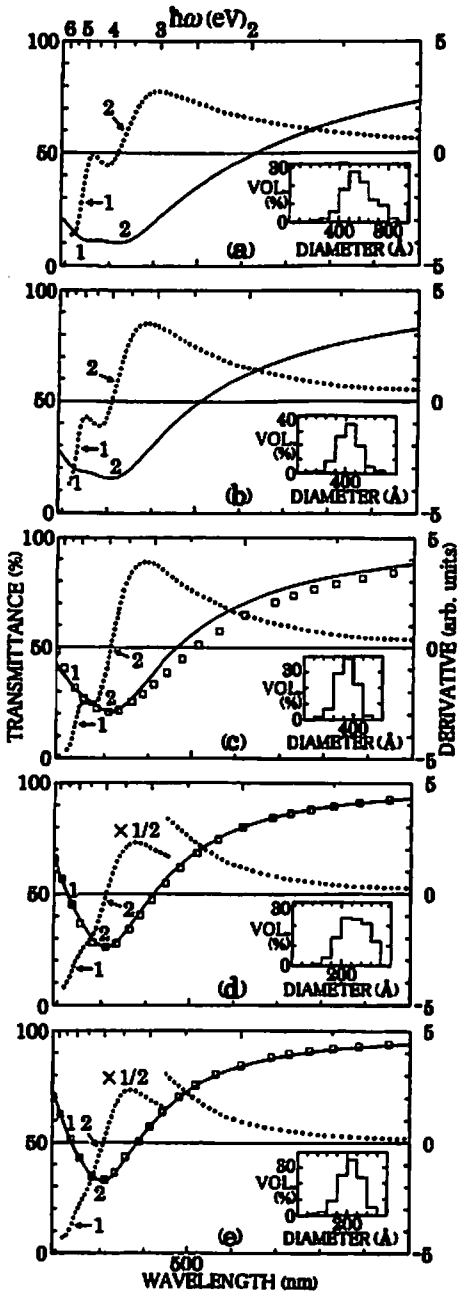

FIG. 2. Experimental transmittance spectra (solid curves) and the derivatives (dotted curves) of indium-island films with particle diameters of about (a) 520, (b) 440, (c) 360, (d) 260, and (e) 220 Å. The weight thicknesses are (a) 116.1, (b) 88.5, (c) 77.4, (d) 55.3, and (e) 44.2 Å. The deposition rates were (a) 0.12, (b) 0.07, (c) 0.11, (d) 0.10, and (e) 0.14 Å/s. The squared curves are the simulated transmittance spectra. In the simulation, the weight thicknesses are (c) 140.4, (d) 80.4, and (e) 58.6 Å, and the effective depolarization factors are (c) 0.198, (d) 0.199, and (e) 0.204.

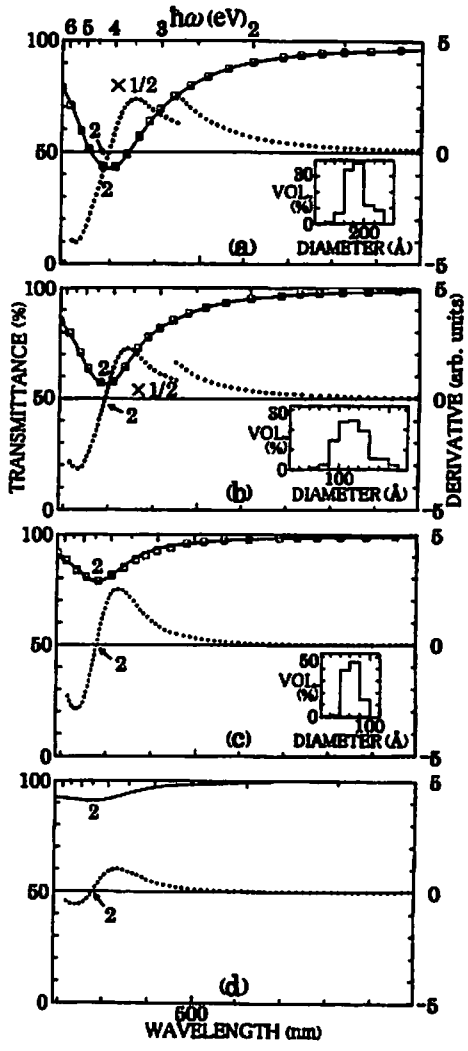

FIG. 3. Experimental transmittance spectra (solid curves) and the derivatives (dotted curves) of indium-island films with particle diameters of about (a) 160, (b) 120, and (c) 60 Å in diameter. The weight thicknesses are (a) 33.2, (b) 22.1, (c) 11.1, and (d) 6.6 Å. The deposition rates were (a) 0.14, (b) 0.13, (c) 0.12, and (d) 0.09 Å/s. The squared curves are the simulated transmittance spectra. In the simulation, the weight thicknesses are (a) 38.8, (b) 21.6, and (c) 9.3 Å, and the effective depolarization factors are (a) 0.214, (b) 0.220, and (c) 0.241.

Figures 3(a)–3(c) show the experimental spectra of the indium-island films with particle diameters of about 160, 120, and 60 Å, respectively. The film of Fig. 3(a) is shown in Fig. 2(b). The particle size for the film of Fig. 3(d) was difficult to investigate using electron microscope because of the low contrast due to the SiO_2 coating. The particle size for the film in Fig. 3(d) is presumably smaller than that for the film of Fig. 3(c) because the particle size becomes smaller with decreasing weight thickness.[13] Only the step for absorption 2 could be found for the derivatives in Fig. 3, in which the position of absorption 2 is (a) 292±6 nm, (b) 289±7 nm, (c) 278±8 nm, and (d) 276±10 nm.

The indium-island films in the present study consist of particles smaller than the wavelength of incident light. Thus, as mentioned in Sec. I, the indium-island films should show interband absorption and/or optical plasma-resonance absorption.

Optical plasma-resonance absorption of metal-island films shifts to a shorter wavelength with decreasing weight thickness[3,4,8] because of the increase in F in Eq. (1). This shift is characteristic of the optical plasma-resonance absorption of metal-island films. As shown in Figs. 2 and 3, absorption 2 is shifted to a shorter wavelength with decreasing weight thickness. Such a shift agrees with the characteristic mentioned above, proving absorption 2 to be optical plasma-resonance absorption.

TABLE I. The particle diameter for the island films of Figs. 2(c)–2(e) and 3(a)–3(c), the full half width Γ of the optical plasma-resonance absorption of these island films, the relaxation time τ of the conduction electrons estimated from Γ, and the mean free path l corresponding to τ. In this table, τ and l for particle sizes of 120 and 160 Å in diameter are nearly the real value. The relaxation time and mean free path of the bulk are also shown.

Diameter (Å)	Γ(eV)	τ ($\times 10^{-16}$ s)	l(Å)
360 [Fig. 2(c)]	2.52	2.62	
260 [Fig. 2(d)]	1.85	3.56	6.19
220 [Fig. 2(e)]	1.96	3.36	5.85
160 [Fig. 3(a)]	1.98	3.33	5.79
120 [Fig. 3(b)]	1.96	3.36	5.85
60 [Fig. 3(c)]	2.49	2.65	
Bulk		38[a]	66.1[b]

[a]Ref. 18.
[b]Bulk τ (Ref. 18) $\times \nu_F$ (Fermi velocity, Ref. 19).

In simple metal particles, the spill-out effect[14] causes optical plasma-resonance absorption to shift to a longer wavelength with decreasing particle size. This shift should occur for indium particles and is in contrast to the shift to a shorter wavelength mentioned above. We consider as follows: the spill-out effect is presumably weak in the indium particles, and thus the shift caused by the increase in F is dominant.

In Fig. 2, the position of absorption 1 is almost constant irrespective of weight thickness. Thus, it is evident that absorption 1 is not optical plasma-resonance absorption but interband absorption. The step for interband absorption weakens when particle size decreases. Consequently, interband absorption becomes weaker with decreasing particle size. The step for interband absorption is not found for the derivatives in Fig. 3. From this, we consider interband absorption to disappear in particle sizes below about 200 Å in diameter [Fig. 2(e)].

C. Simulation of optical plasma-resonance absorption

We simulated optical plasma-resonance absorption with the Maxwell-Garnett-type EMT, taken into account in Eq. (1), as follows. The second term of the right side of Eq. (1) gives the absorption spectrum. We can obtain the value of this term by applying Eq. (1) to the spectrum, and then from the position for half of the peak of the optical plasma-resonance absorption we can evaluate the full half width Γ. For the spectra in Figs. 2(c)–2(e) and 3(a)–3(c), we could evaluate Γ [Table I (eV unit)].

As previously mentioned,[5] the relaxation time τ of conduction electrons was estimated from $\Gamma(=\tau^{-1})$ in Table I. We simulated optical plasma-resonance absorption by using the estimated τ values for Eqs. (1)–(3). $\omega_p(\hbar\omega_p = 12.6$ eV) calculated from the equation in Ref. 15 was used because there is very little data on ω_p of indium particles. As was often done in earlier studies, the values of d_w and F in Eq. (1) were chosen to match the experimental peak and its position, respectively. n_i and n_s in Eq. (1) were taken to be constant at 1.47 of SiO_2, and ε_a in Eq. (2) was taken to be constant at 2.17 of SiO_2, by considering the fused-quartz substrate and the SiO_2 coating (Sec. III) and by referring to the values in Refs. 3, 4, and 16. The squared curves in Figs. 2(c)–2(e) and 3(a)–3(c) show the simulated optical plasma-resonance absorption.

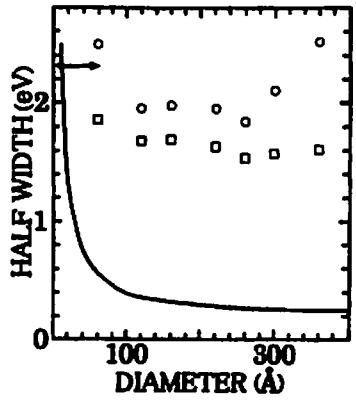

FIG. 4. The half width of the optical plasma-resonance absorption against the particle diameter. ○ full half width Γ; □ half width $2\Gamma_{1/2}$; ↔ the particle size range for $2\Gamma_{1/2}$ of the film of Fig. 3(d). The solid curve is the full half width based on the classical size-effect theory of the conduction-electron scattering for spherical particles.

We could not evaluate Γ in Figs. 2(a) and 2(b) because the peak of the optical plasma-resonance absorption could not be determined due to the strong overlap with the interband absorption. Γ was difficult to evaluate in Fig. 3(d) because the position for Γ was out of the spectral range at the shorter-wavelength flank.

D. Half width

Γ was plotted against particle diameter in Fig. 4. The half width $2\Gamma_{1/2}$, where $\Gamma_{1/2}$ is half of Γ at the longer-wavelength flank, was also plotted. $2\Gamma_{1/2}$ for particle sizes of about 360, 260, 220, 160, 120, and 60 Å in diameter was 1.62, 1.54, 1.64, 1.70, 1.68, and 1.86 eV, respectively. $2\Gamma_{1/2}$ in Fig. 3(d) was 2.32 eV. Γ (2.11 eV) and $2\Gamma_{1/2}$ (1.58 eV) for particle sizes of about 300 Å in diameter were also plotted, though the spectrum is not given in this paper. The difference between Γ and $2\Gamma_{1/2}$ was large in particle sizes of about 300 and 360 Å in diameter, showing the overlap with the interband absorption at the shorter-wavelength flank to be strong.

The solid curve in Fig. 4 shows the full half width of the optical plasma-resonance absorption based on Eqs. (1)–(3) and on the classical size-effect theory[17] of the conduction-electron scattering for spherical particles. In the classical size-effect theory, the full half width is expressed as[17]

$$\hbar \times (\tau_{\text{bulk}}^{-1} + \nu_F/R), \tag{4}$$

where $\tau_{\text{bulk}}(0.38 \times 10^{-14}$ s) (Ref. 18) is the bulk relaxation time, $\nu_F(1.74 \times 10^8$ cm/s) (Ref. 19) the Fermi velocity, and R the particle radius. The term ν_F/R arises from the scattering of conduction electrons at the particle surface.

In island films, the particle growth due to the agglomeration of smaller particles causes the particle shapes to be irregular.[8,13] We used Eq. (4) because the expression for the half width of optical plasma-resonance absorption has not been reported for irregular-shaped particles.

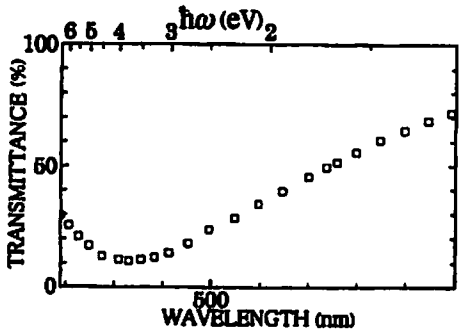

FIG. 5. The simulated transmittance spectrum based on the modified dielectric constant of bulk indium. This spectrum corresponds to the spectrum in Fig. 2(a). In the simulation, the weight thickness is 301.9 Å and the effective depolarization factor is 0.145.

V. DISCUSSION

A. Comparison with previous data

Several authors[20] have studied the optical absorption of bulk indium and found interband absorption at about 207 and 885 nm. Based on the dielectric constant $\varepsilon_{\mathrm{In}}$ of bulk indium[21] and on Eqs. (1) and (2), we investigated the interband absorption previously found[20] as follows.

As with other metals, $\varepsilon_{\mathrm{In}}$ consists of the Drude term ε_f, given by Eq. (3), and the interband-transition term $\delta\varepsilon_b(\varepsilon_{\mathrm{In}} = \varepsilon_f + \delta\varepsilon_b)$. We modified $\varepsilon_{\mathrm{In}}$ by substituting τ (3.36×10^{-16} s) in particles of about 120 Å in diameter (Table I) for the bulk τ (0.38×10^{-14} s)[18] in ε_f. τ in this size is later shown to be nearly the real value. Using the modified $\varepsilon_{\mathrm{In}}$ for Eqs. (1) and (2), we simulated the spectrum (Fig. 5). The values of d_w and F were chosen to match the peak and its position in Fig. 2(a), respectively. This simulated spectrum is composed of bulk interband-absorption and optical plasma-resonance absorption corresponding to that of particles of about 120 Å in diameter [Fig. 3(b)].

Similar to the case in Fig. 2(a), interband absorption was not found at about 885 nm in Fig. 5. From this, we see that interband absorption at about 885 nm is very weak and thus difficult to detect because of the overlap with the optical plasma-resonance absorption. The presence of interband absorption at about 207 nm is not clear in Fig. 5. However, notable interband absorption is found at about 235 nm in Fig. 2(a). We consider that the interband absorption at about 235 nm in Fig. 2(a) corresponds to the interband absorption at about 207 nm in a previous study.[20] We could not clarify the reason for the difference in the position.

B. Interband absorption

In noble and transition metal particles,[22] when lattice constants contract with decreasing particle size, interband absorption shifts to a shorter wavelength and then disappears below a particle size. In the present study, lattice contraction was not found (Sec. IV A). Thus, the disappearance in particle sizes below about 200 Å in diameter is not caused by the lattice contraction.

There is very little data on energy bands, which can identify the transition for interband absorption at about 234 nm in Fig. 2. In the present study, thus, interband absorption was difficult to investigate referring to energy bands.

For example, in bulk copper,[23,24] compared to the DOS of the $3d$ bands of the bulk, the DOS of the $3d$ bands of the surface layer is small at the lower portion and large at the upper portion. This is because the coordination number is lower for surface atoms than for bulk atoms. The DOS of the bands of metal particles should change from a bulklike state to a surface-layer-like state with decreasing particle size, because the ratio of surface to volume atoms increases with decreasing particle size. Thus, the DOS of the bands of the metal particles decreases at the lower portion and increases at the upper portion with decreasing particle size.

One of the conditions of occurrence of interband absorption, due to transitions between the initial and final bands, is that the DOS for the initial band is large. In metal particles, if the initial band is present at the lower portion of the bands, interband absorption should weaken or disappear with decreasing particle size because of the DOS decrease at the lower portion. In this case, when the DOS decrease is small, the shift of the position of the initial band is unremarkable and thus the position of the interband absorption remains almost constant.[2]

In the lead particles,[2] interband absorption, the initial band for which is positioned at the bottom of the conduction bands, disappears in particle sizes below about 300 Å in diameter and its position remains almost constant (at about 288 nm) before the disappearance. The disappearance and the almost constant position have been ascribed to the DOS decrease mentioned above.

At present, only the interband absorption of the lead particles is similar to that of indium particles; i.e., in both cases the position is almost constant before disappearance below a certain particle size. This similarity suggests that as in the lead particles the initial band is positioned at the bottom of the conduction bands and the disappearance results from the DOS decrease based on the low coordination number of surface atoms.

C. Optical plasma-resonance absorption

1. Practically no influence from distributions of particle shape and size

In a metal particle, the depolarization factor and the spill-out effect (Sec. III B), dependent on the particle shape[25] and size,[14] respectively, affect the peak position of optical plasma-resonance absorption. Thus, in a metal-island film with distributions of particle shape and size, the peak positions for metal particles are distributed. Equations (1)–(3) do not apply to such metal-island film. The scattering of conduction electrons in a metal particle causes a broadening (i.e., a damping) of optical plasma-resonance absorption of the metal particle. If the scattering depends on the particle size, the broadening must be size dependent. In this case, when a metal-island film has particle-size distribution, the broadening for metal particles is distributed. Equations (1)–(3) do not apply to such metal-island film. It seems that the particle shapes are not uniform in Fig. 1, and the particle-size distribution is shown in Figs. 2 and 3.

When metal-island film shows a spectrum in which the optical plasma-resonance absorption overlaps the interband absorption, we cannot simulate the spectrum by Eqs. (1)–(3) because the interband absorption is not taken into account.

From this discussion, if Γ used in the simulation in Sec. IV C includes the contribution from the distributions of the particle shape and size and from the overlap with the interband absorption, the simulated spectrum in Sec. IV C, based on Eqs. (1)–(3), should not fit the experimental spectrum.

In particle sizes of about 360 Å in diameter [Fig. 2(c)], the fit to the experimental spectrum is not good. As mentioned above, the possible causes are the distributions of the particle shape and size and the overlap with interband absorption. In particle sizes of about 260 [Fig. 2(d)] and 220 Å in diameter [Fig. 2(e)], the fit is slightly not good. The possible causes are still the distributions and the overlap. The fit is good in particle sizes of about 160 [Fig. 3(a)] and 120 Å in diameter [Fig. 3(b)]. Interband absorption disappears in these particle sizes (Sec. IV B). Thus, in particle sizes of about 120 and 160 Å in diameter with good fit, practically no influence from the distributions of the particle shape and size is shown. From good fit, it can be seen that the constant values of n_i, n_s, and ε_a used in the simulation are valid.

With practically no influence from the particle-shape distribution, it can be seen that this distribution is small. This seems to be because indium particles of about 120 and 160 Å in diameter are formed at an early stage of the particle growth due to the agglomeration of smaller particles.[8,13] At this stage, variety of particle shapes is small. With practically no influence from the particle-size distribution, it can be seen that the spill-out effect is weak and that the conduction-electron scattering is not size dependent. This weak spill-out effect agrees with that mentioned in Sec. IV B, but it was difficult to clarify the reason why the spill-out effect is weak. The conduction-electron scattering is discussed below.

2. Relaxation time and mean free path of conduction electrons

With practically no influence from the particle-shape distribution together with the weak spill-out effect, it can be seen that the broadening of the optical plasma-resonance absorption in particle sizes of about 120 and 160 Å in diameter is mainly due to conduction-electron scattering which is not dependent on particle size. Thus, τ in particle sizes of about 120 and 160 Å in diameter, which is nearly the real value because the fit is good, is based on such conduction-electron scattering.

In the present study, τ is related to the mean free path l as follows:

$$l = v_F \times \tau \tag{5}$$

Applying Eq. (5) to τ in particle sizes of about 120 and 160 Å in diameter (Table I) and using v_F (Ref. 19), we estimated l to be 5.85 and 5.79 Å (Table I).

τ and l estimated above are much smaller than the bulk values (Table I) but comparable to those (about 3.8×10^{-16} s and 8 Å) of aluminum particles.[3,4] The indium particles in the present study are polycrystalline (Sec. IV A). Thus, as with aluminum particles,[3,4] we attribute the much smaller τ and l to the scattering of conduction electrons at lattice defects within the particles. This implies that indium particles of about 120 and 160 Å in diameter have a higher lattice-defect density than bulk indium and that at these sizes the scattering at lattice defects is dominant in conduction-electron scattering. The scattering at lattice defects internal to the particles does not depend on particle size. Thus, particle-size distribution is practically of no influence in the case of good fit.

A lot of literature exists on the damping mechanism of the optical plasma-resonance absorption of metal particles.[26] However, in such literature, the damping is particle-size dependent. Thus, at present, only scattering at lattice defects can qualitatively explain why particle-size distribution has practically no influence.

3. Size-dependent broadening

In Fig. 4, in particle sizes below about 100 Å in diameter $2\Gamma_{1/2}$ increases with decreasing particle size. Γ in particle sizes of about 60 Å in diameter is larger than that of about 120 and 160 Å in diameter. Thus, similar to $2\Gamma_{1/2}$, in particle sizes below about 100 Å in diameter Γ should increase with decreasing particle size. The conduction-electron scattering consists of electron-phonon scattering, electron-electron scattering, electron-lattice defect scattering, and electron-particle surface scattering.[10] Thus, scattering at the particle surface also occurs when the scattering at lattice defects is dominant.[10] In Fig. 4, the solid curve for spherical particles notably increases in particles sizes below about 100 Å in diameter, showing that the scattering at the particle surface notably increases below this size. Thus, if indium particles are almost spherical in particle sizes below about 100 Å in diameter, the notable increase in the scattering at the particle surface may be responsible for the increase in $2\Gamma_{1/2}$ and Γ in particle sizes below about 100 Å in diameter. It was difficult to investigate the size-dependent increase in $2\Gamma_{1/2}$ and Γ further.

The size-dependent increase in Γ shows that Γ, in particle sizes below about 100 Å in diameter, includes the contribution of the particle-size distribution. Thus, τ used in the simulation in particle sizes of about 60 Å in diameter [Fig. 3(c)] is not nearly the real value. The fit to the experimental spectrum is not good in particle sizes of about 60 Å in diameter [Fig. 3(c)]. A possible cause is such τ.

D. Effect of disorder in particle distribution and interactions with SiO_2

Theoretical studies[27] of randomly distributed metal particles have reported that the disorder in the distribution causes the optical plasma-resonance absorption to be broad and asymmetric. The good fit in particle sizes of about 160 [Fig. 3(a)] and 120 Å in diameter [Fig. 3(b)] shows the optical plasma-resonance absorption to be symmetric. Thus, the disorder has little influence on the optical plasma-resonance absorption for good fit.

For silver particles embedded in the SiO_2 matrix, the influence of the interaction between the particles and the matrix on the broadening of optical plasma-resonance absorp-

tion has been reported in theory.[28] In this interaction, the broadening is particle-size dependent. Practically no influence from the particle-size distribution (Sec. V C 1) shows that the broadening is not particle-size dependent. Thus, such interaction does not occur in indium-island films for good fit.

If electrons of the SiO_2 matrix occupy the final state of the interband transition of the indium particles, the transition would be restricted and thus the interband absorption would disappear. Here the indium particles are assumed to have Fermi energy the same as that of bulk indium, because there is very little data on the Fermi energy of indium particles. The Fermi energy of the indium particles is about 3.1 eV higher than that of bulk silver,[19] and the Fermi energy of bulk silver is about 6.3 eV higher than the valence-band maximum of SiO_2.[28] From these values, the Fermi energy of the indium particles is much higher (about 9.4 eV) than the valence-band maximum of SiO_2. Thus, the valence band of SiO_2 does not overlap the final state lying at values higher than the Fermi energy, i.e., the electrons of the SiO_2 matrix cannot occupy the final state. This shows that occupation of the final state is not the cause of the disappearance of the interband absorption.

VI. SUMMARY

We studied the optical absorption of indium particles experimentally. The interband absorption, the position of which remains almost constant (at about 234 nm) irrespective of particle size, disappeared in particle sizes below about 200 Å in diameter. This disappearance is similar to that in lead particles, where the disappearance originates from the DOS decrease based on the low coordination number of surface atoms. The similarity suggests that the cause of the disappearance is the same as that in the lead particles.

We investigated the relaxation time τ and the mean free path l of conduction electrons by simulating the optical plasma-resonance absorption with the Maxwell-Garnett-type EMT. τ and l in particle sizes of about 120 and 160 Å in diameter are estimated to be $(3.33–3.36)\times 10^{-16}$ s and 5.79–5.85 Å, respectively, which is much smaller than the bulk values (0.38×10^{-14} s and 66.1 Å). Referring to the presence of lattice defects in the indium particles and to the studies of the aluminum particles, we ascribed the small τ and l to the scattering of conduction electrons at lattice defects within the particles.

The optical absorption of indium particles smaller than about 100 Å in diameter still needs to be studied in relation to the crystal structure, because the crystal structure of these particles was assumed to be the same as that of the bulk indium.

ACKNOWLEDGMENTS

We are grateful to Professor Masayuki Ido (Hokkaido University) for his valuable comments and encouragement throughout this work. One of us (E.A.) is greatly indebted to Professor Tomuo Yamaguchi (Shizuoka University) for his useful suggestions and informative discussions.

[1]See, for example, J. A. Creighton and D. G. Eadon, J. Chem. Soc., Faraday Trans. **87**, 3881 (1991).
[2]E. Anno and M. Tanimoto, Phys. Rev. B **66**, 165442 (2002).
[3]H. V. Nguyen, I. An, and R. W. Collins, Phys. Rev. B **47**, 3947 (1993).
[4]H. V. Nguyen and R. W. Collins, J. Opt. Soc. Am. A **10**, 515 (1993).
[5]E. Anno and M. Tanimoto, Phys. Rev. B **64**, 165407 (2001).
[6]S. Yoshida, T. Yamaguchi, and A. Kinbara, J. Opt. Soc. Am. **62**, 1415 (1972).
[7]See, for example, M. Born and E. Wolf, *Principles of Optics*, 5th ed. (Pergamon, New York, 1975), p. 61; T. Yamaguchi, H. Takahashi, and A. Sudoh, J. Opt. Soc. Am. **68**, 1039 (1978), and references therein.
[8]T. Yamaguchi, S. Yoshida, and A. Kinbara, Thin Solid Films **18**, 63 (1973); **21**, 173 (1974).
[9]See, for example, N. W. Ashcroft and N. D. Mermin, *Solid State Physics* (Saunders, Philadelphia, 1976), p. 17.
[10]U. Kreibig, Z. Phys. B **31**, 39 (1978); E. Anno and R. Hoshino, J. Phys. Soc. Jpn. **50**, 1209 (1981).
[11]Y. Oshima, T. Nangou, H. Hirayama, and K. Takayanagi, Surf. Sci. **476**, 107 (2001).
[12]M. Cardona, *Modulation Spectroscopy* (Academic, New York, 1969), pp. 105–115.
[13]D. W. Pashley, M. J. Stowell, M. H. Jacobs, and T. J. Law, Philos. Mag. **10**, 127 (1964).
[14]A. Liebsch, *Electronic Excitations at Metal Surfaces* (Plenum, New York, 1997), pp. 130–141, and references therein.
[15]N. W. Ashcroft and N. D. Mermin, in Ref. 9, p. 38 and 758.
[16]*American Institute of Physics Handbook*, 3rd ed., edited by D. E. Gray (McGraw-Hill, New York, 1972), Sec. 6, p. 13 and 28. In this reference, the refractive index of fused quartz is almost constant (1.4–1.5) in the spectral range of the present study.
[17]See, for example, U. Kreibig and C. V. Fragstein, Z. Phys. **224**, 307 (1969), and references therein.
[18]N. W. Ashcroft and N. D. Mermin, in Ref. 9, p. 10.
[19]C. Kittel, *Introduction to Solid State Physics*, 6th ed. (Wiley, New York, 1986), p. 134.
[20]See, for example, R. Y. Koyama, N. V. Smith, and W. E. Spicer, Phys. Rev. B **8**, 2426 (1973), and references therein.
[21]*Handbook of Optical Constants of Solids III*, edited by E. D. Palik (Academic, New York, 1998), p. 267 and 268.
[22]See, for example, E. Anno, Surf. Sci. **260**, 245 (1992); E. Anno and T. Yamaguchi, Phys. Rev. B **55**, 4783 (1997).
[23]J. A. Appelbaum and D. R. Hamann, Solid State Commun. **27**, 881 (1978).
[24]J. G. Gay, J. R. Smith, and F. J. Arlinghaus, Phys. Rev. Lett. **42**, 332 (1979); J. R. Smith, J. G. Gay, and F. J. Arlinghaus, Phys. Rev. B **21**, 2201 (1980).
[25]See, for example, S. Yamaguchi, J. Phys. Soc. Jpn. **15**, 1577 (1960).
[26]See, for example, U. Kreibig and L. Genzel, Surf. Sci. **156**, 678 (1985), and references therein.
[27]B. N. J. Persson and A. Liebsch, Phys. Rev. B **28**, 4247 (1983); A. Liebsch and P. V. González, *ibid.* **29**, 6907 (1984).
[28]B. N. J. Persson, Surf. Sci. **281**, 153 (1993), and references therein.